This article was downloaded by: [Siauliu University Library]
On: 17 February 2013, At: 06:51
Publisher: Taylor & Francis
Informa Ltd Registered in England and Wales Registered Number: 1072954
Registered office: Mortimer House, 37-41 Mortimer Street, London W1T 3JH, UK

Advanced Composite Materials
Publication details, including instructions for authors and subscription information:
http://www.tandfonline.com/loi/tacm20

Three-Point Flexural Behaviour of GFRP Sandwich Composites: A Failure Map

A. Valenza [a] , V. Fiore [b] & L. Calabrese [c]

[a] Dipartimento di Ingegneria Chimica dei Processi e dei Materiali, University of Palermo, Viale delle Scienze, 90128 Palermo, Italy;, Email: valenza@dicpm.unipa.it

[b] Dipartimento di Ingegneria Chimica dei Processi e dei Materiali, University of Palermo, Viale delle Scienze, 90128 Palermo, Italy

[c] Dipartimento di Chimica Industriale e Ingegneria dei Materiali, University of Messina, Salita Sperone 31, 98166 S. Agata di Messina, Italy

Version of record first published: 02 Apr 2012.

To cite this article: A. Valenza , V. Fiore & L. Calabrese (2010): Three-Point Flexural Behaviour of GFRP Sandwich Composites: A Failure Map, Advanced Composite Materials, 19:1, 79-90

To link to this article: http://dx.doi.org/10.1163/092430409X12530067339280

PLEASE SCROLL DOWN FOR ARTICLE

Full terms and conditions of use: http://www.tandfonline.com/page/terms-and-conditions

This article may be used for research, teaching, and private study purposes. Any substantial or systematic reproduction, redistribution, reselling, loan, sub-licensing, systematic supply, or distribution in any form to anyone is expressly forbidden.

The publisher does not give any warranty express or implied or make any representation that the contents will be complete or accurate or up to date. The accuracy of any instructions, formulae, and drug doses should be independently verified with primary sources. The publisher shall not be liable for any loss, actions, claims, proceedings, demand, or costs or damages whatsoever or

howsoever caused arising directly or indirectly in connection with or arising out of the use of this material.

Downloaded by [Siauliu University Library] at 06:51 17 February 2013

VSP

Advanced Composite Materials 19 (2010) 79–90

ADVANCED COMPOSITE MATERIALS
brill.nl/acm

Three-Point Flexural Behaviour of GFRP Sandwich Composites: A Failure Map

A. Valenza [a,*], **V. Fiore** [a] **and L. Calabrese** [b]

[a] Dipartimento di Ingegneria Chimica dei Processi e dei Materiali, University of Palermo, Viale delle Scienze, 90128 Palermo, Italy

[b] Dipartimento di Chimica Industriale e Ingegneria dei Materiali, University of Messina, Salita Sperone 31, 98166 S. Agata di Messina, Italy

Received 21 October 2008; accepted 18 February 2009

Downloaded by [Siauliu University Library] at 06:51 17 February 2013

Abstract

In this work, the failure mechanisms of GFRP/PVC foam core sandwich structures subjected to three-point bending are analysed.

By varying the skin thickness (t) and the span length between supports (l), experimental tests were carried out in order to find the relationship between the geometrical configuration of the sandwiches and the failure mechanism.

By plotting failure mechanism on a graph of l against t, a failure map was created identifying the three typical failure mode regions of these sandwiches. The graph clearly shows the failure mode corresponding to each combination of l and t.

To help optimise the use of these sandwich beams as structural elements, a theoretical failure mode map was constructed. The theoretical model results were consistent with the experimental ones, and so we can conclude that the theoretical model is a reliable predictor of failure mechanisms in sandwiches with defined geometry.

© Koninklijke Brill NV, Leiden, 2010

Keywords

Sandwich, failure mechanism, three-point bending, failure map

1. Introduction

In recent years, numerous studies have been carried out to find lighter structures with better mechanical performance. Composite sandwiches are an excellent compromise when an optimal trade-off between light weight and high performance is required.

* To whom correspondence should be addressed. E-mail: valenza@dicpm.unipa.it

© Koninklijke Brill NV, Leiden, 2010

DOI:10.1163/092430409X12530067339280

Consequently these structures are being increasingly used in many industrial fields such as shipbuilding, automotive and civil structures [1, 2]. Their excellent strength, stiffness and lightness make them a very useful tool for designers.

Sandwich materials consist of two thin, stiff and strong outer skins enclosing a thick, lightweight core. Commonly used materials for the skins are composite laminates and metals, while the core is usually made of metallic and non-metallic honeycombs, cellular foams or balsa wood [3]. The core may be bonded to the skins with adhesives or by using the resin in the skins as a binder. By separating the skins through a low density core, the moment of inertia of the panel is increased so increasing bending stiffness.

Many researchers have investigated the relationship between the failure mechanisms, the type of material used and the geometrical configuration of sandwich structures when subjected to three-point bending.

Steeves and Fleck [4] devised a systematic procedure to compare the performance of sandwich beams with various combinations of materials. They identified the operative failure mechanisms and optimised the geometry of the sandwich structures to minimise the mass for a given load-bearing capacity.

Petras and Sutcliffe [5] studied the failure mechanisms for GFRP skins/honeycomb core sandwich beams. They then constructed a failure mode map showing the dependence of failure mode and load on skin thickness to span length ratio and honeycomb density.

The aim of this work is to understand how geometrical configuration affects failure mechanism for GFRP/PVC foam core sandwich structures subjected to three-point bending.

All structures tested in this work had an E-glass/epoxy composite skin and closed-cell PVC foam core and were produced by vacuum bagging.

These kinds of sandwich structures are currently being used in small, non-structural components of boats to minimise the total weight. Specific examples include shower trays, battery boxes, internal elements of hatches and bathroom furniture in general.

By varying the skin thickness (t) and the span length between support (l) experimental tests were carried out. From these results an experimental failure mode map of l against t was created.

To optimise the use of these sandwich beams as structural elements, a theoretical failure mode map was constructed. The theoretical results tallied with the experimental ones and consequently it was shown that the theoretical model is a reliable predictor of failure mechanisms in composite sandwiches with defined geometry.

2. Consideration of Collapse Modes

When a sandwich structure is subjected to three-point bending, several failure mechanisms may occur.

Downloaded by [Siauliu University Library] at 06:51 17 February 2013

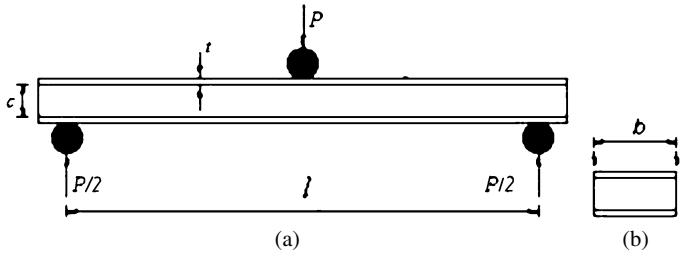

Figure 1. Schematic diagram of the three-point bending test: (a) loading configuration and (b) cross section.

Downloaded by [Siauliu University Library] at 06:51 17 February 2013

In literature, five main failure mechanisms are identified: skin compressive/ tensile failure, core shear failure, skin wrinkling, indentation and delamination, i.e., skin-core debonding.

In the case of the load configuration shown in Fig. 1, a sandwich beam is subjected to a bending moment M and shear load V. For relatively thin skins and relatively low core stiffness, the bending moment is mainly taken up by the skins, while the shear stress is mainly taken up by the core.

Compressive or tensile skin failure happens when the axial stress reaches the tensile (or compressive) strength of lower (or upper) skin.

The compressive or tensile skin stress, σ_f, is given by [6]:

$$\sigma_f = \frac{M}{b \cdot t \cdot (t + c)} \cong \frac{M}{b \cdot t \cdot c}. \tag{1}$$

As the maximum bending moment is given by $M = (P \cdot l)/4$, the value of the failure load is described by:

$$P_{SC/T} = \frac{4 \cdot b \cdot t \cdot c \cdot \sigma_f}{l}. \tag{2}$$

Core shear failure mode occurs when the core shear strength is exceeded by the shear stress.

The equation for shear stress τ_c in the core is [6]:

$$\tau_c = \frac{V}{b \cdot (t + c)} \approx \frac{V}{b \cdot c}. \tag{3}$$

Since shear is given by $V = P/2$, the peak load is described by the following expression:

$$P_{CS} = 2 \cdot b \cdot c \cdot \tau_C. \tag{4}$$

Skin wrinkling is defined as a localized short-wavelength buckling of the upper skin. Wrinkling is the buckling of the skin under compression (upper) supported on one side by an elastic or elasto-plastic element (the core).

The critical wrinkling load is a function of core stiffness, skins stiffness, the geometry of the beam and the applied load [7].

The value of the fracture load is given by [8]:

$$P_{\mathrm{W}} = \frac{4 \cdot b \cdot t \cdot c}{l} \cdot 3 \cdot \left[\frac{E_{\mathrm{f}} \cdot E_{\mathrm{C}}^2}{12 \cdot (3 - \nu_{\mathrm{C}})^2 \cdot (1 + \nu_{\mathrm{C}})^2} \right]^{1/3}, \tag{5}$$

where ν_{C} is the Poisson's ratio of the core, E_{f} is the Young's modulus of the skin and E_{C} is the compressive modulus of the core.

Indentation happens when the load is highly localised and exceeds the core compression strength. This failure mechanism occurs at points of concentrated load, such as fittings, corners or joints. Practically speaking, failure of this type can be avoided by applying the load over a sufficiently large area [9].

In recent years, many researchers [4, 10–14] have focused their attention on this particular failure mechanism.

Debonding is failure at the interface zone between the core and the skin. Even knowing the mechanical characteristics of the skin and the core it is very difficult to perform theoretical strength prediction analysis for this failure mechanism.

3. Experimental Setup

3.1. Materials and Manufacturing

Four symmetrical sandwiches were produced by vacuum bagging. This method involves an initial hand lay-up phase and the polymerization of laminate matrix in a flexible vacuum bag in which negative pressure is reached by a vacuum pump.

The structures prepared consisted of a common PVC foam core and a GFRP skin with one (called 'M1'), two ('M2'), three ('M3') and four layers ('M4'), respectively.

The core was made from 'closed cell' PVC foam (Herex® C 70.55 from Alcan composites) with thickness $c = 5$ mm and density 60 kg/m^3. Herex® C 70.55 has a compressive strength of 0.85 MPa, compressive modulus of 58 MPa, shear strength of 0.8 MPa and shear modulus of 22 MPa.

The sandwich skins were produced with E-glass mat (random fibres with an areal density of 0.3 kg/m^2).

A SR 8100 DGEBA epoxy resin mixed with the hardener SD 8822, both supplied by Sicomin, was used as the matrix material. This mix gives a matrix with a tensile strength of 70 MPa, tensile modulus of 3 GPa, flexural strength of 115 MPa and flexural modulus of 3.39 GPa.

3.2. Mechanical Testing

For each sandwich, three-point flexure tests were carried out with span distance l equal to 40, 50, 60, 80, 100, 120, 140, 160, 180 and 200 mm respectively.

Flexural tests were performed on prismatic samples (see Fig. 1) with width $(b) =$ 15 mm, total length $(L) = l + 50$ mm and variable skin thickness (t). To be precise, t varied between 0.257 mm and 0.376 mm for the 'M1' samples, between 0.849 mm

Downloaded by [Siauliu University Library] at 06:51 17 February 2013

and 1.128 mm for the 'M2' samples, between 1.471 mm and 1.823 mm for the 'M3' samples and between 2.268 mm and 2.517 mm for the 'M4' samples.

The thickness of skins in the single layer M1 sandwiches is much smaller than the equivalent thickness of one single layer of the other multilayer skins (M2, M3, and M4). This is due to the nature of the vacuum bagging method of manufacture. The compaction pressure applied during the process extracts surplus resin much more efficiently from a single layer sandwich than from a multilayer sandwich. As a consequence, the multilayer sandwiches have higher resin content than M1 sandwiches and so are thicker 'per layer'.

Samples were tested using a Universal Testing Machine (UTM) mod. 3365 by Instron, equipped with a load cell of 5 kN, with a speed of 1 mm/min and repeated five times for each sample type.

Downloaded by [Siauliu University Library] at 06:51 17 February 2013

4. Results and Discussion

4.1. Failure Mode Observations

The experimental mechanical tests show that, for the sandwich structures analysed in this paper, only three failure mechanisms actually occur.

By observing the results shown in Figs 2–4, it is clear that two of the mechanisms can be defined as indentation failures and the third as a tensile failure of the lower skin. For ease of identification we will call the indentation failures 'indentation type I' and 'indentation type II', respectively.

In the case of indentation type I (see Fig. 2), the core yields under the localised load without skin failure. This is a non-catastrophic failure mechanism due to progressive collapse of the cell structure of the foam.

At the point of load application, foam densification takes place due to the initial buckling fracture of the cell walls in the PVC core. This results in a significant reduction in the local thickness of the sandwich. At large deflections a lower skin fracture appears.

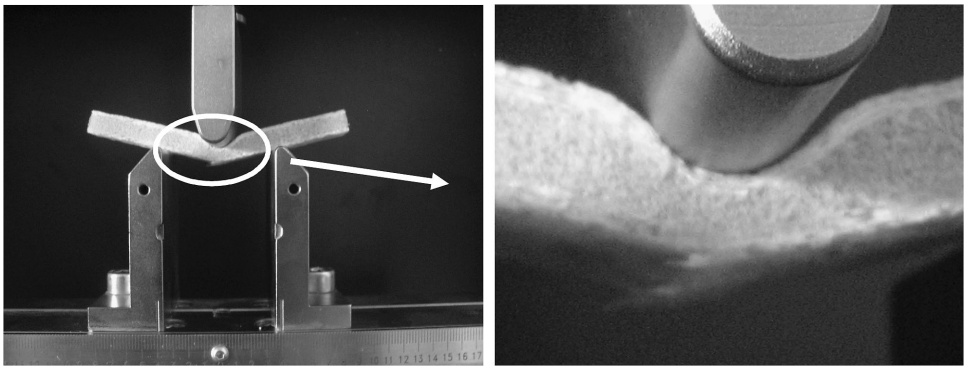

Figure 2. Photograph of the 'non catastrophic' indentation failure called 'indentation type I' for sandwich under three point flexural test.

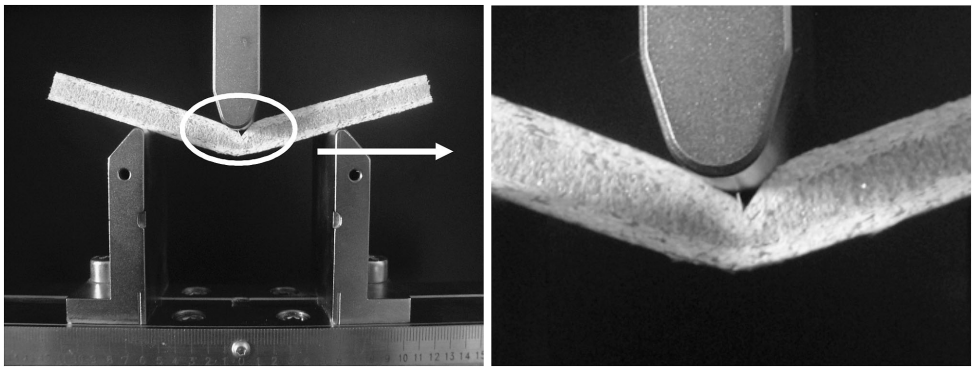

Figure 3. Photograph of the 'catastrophic' indentation failure called 'indentation type II' for sandwich under three point flexural test.

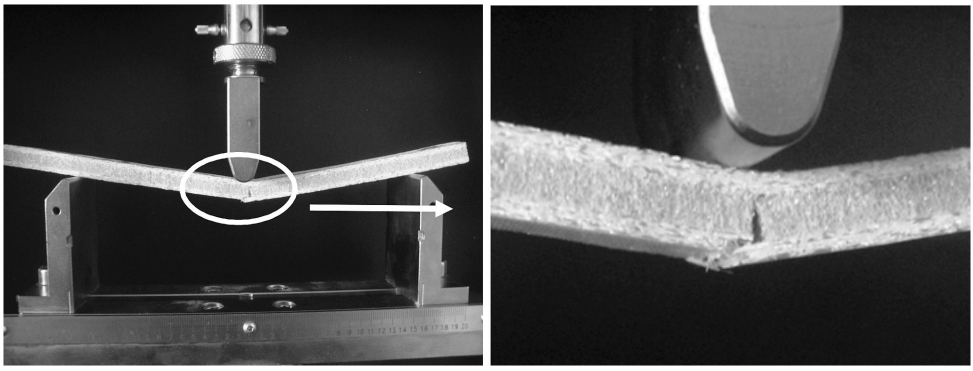

Figure 4. Photograph of the tensile skin failure for sandwich under three point flexural test.

When indentation type II failure (see Fig. 3) occurs, the locally applied load significantly deforms the upper skin until it eventually collapses. No delamination was observed at the skin–core interface in any of the experiments.

In the case of tensile skin failure (Fig. 4), the crack starts in the lower skin and typically propagates along the lower skin–core interface for a short distance. It subsequently moves across the core until it reaches the interface between the core and the upper skin of the structure.

In this research, the thickness c of the core was fixed at 5 mm and so the influence of this parameter on failure modes was not analysed. With increasing thickness (c) it is likely that other failure modes, such as core shear failure and skin wrinkling, will occur. The influence of core thickness on the failure modes of a sandwich composite is, therefore, a promising area for further research.

4.2. Flexural Tests at Varying the Parameter 'I'

Flexural tests results (peak load and failure mode evidenced) are reported in Fig. 5.

Downloaded by [Siauliu University Library] at 06:51 17 February 2013

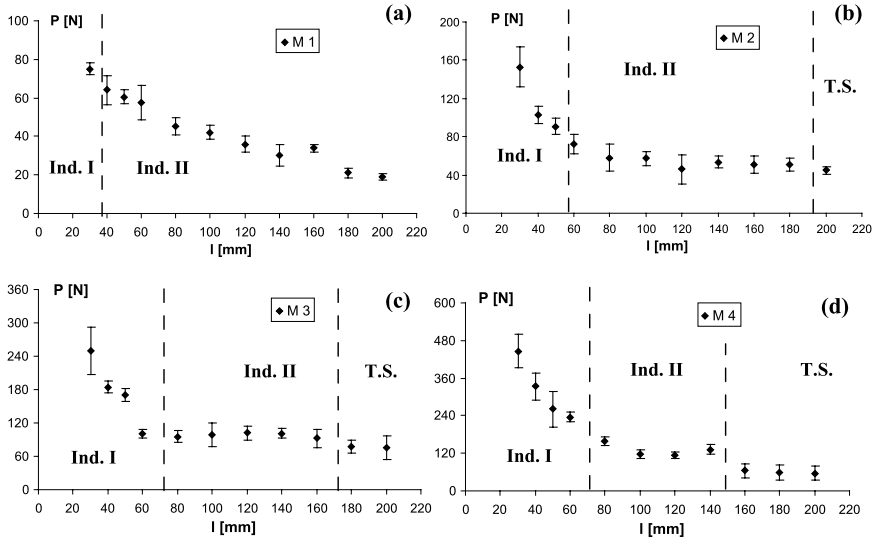

Figure 5. Trends of the maximum load at varying 'l' for samples M1 (a), M2 (b), M3 (c) and M4 (d) evidencing the failure mechanism. Ind. I: indentation type I; Ind. II: indentation type II; T.S.: tensile skin failure.

From Fig. 5(a), we see that the 'M1' sandwiches (one layer of skin) show only indentation type II fractures except for the samples with $l = 30$ mm which has an indentation type I failure. Increasing the span, l, results in a reduction in peak load, P.

The 'M2' sandwiches (two layers of skin) exhibit indentation type I fractures for values of l less than 60 mm and indentation type II failures for all other samples except $l = 200$ mm where tensile skin failure occurs. The peak load, P decreases with increasing l for the samples with indentation type I failures yet actually remains constant when indentation type II failures occur (Fig. 5(b)).

The 'M3' sandwiches (three layers of skin) fail by indentation type I for l values less than 80 mm, indentation type II for l between 80 mm and 160 mm, and tensile skin failure for l greater than 160 mm. For the indentation type I failures, peak load, P, decreases with increasing l. For higher values of l, P maintains constant values, as shown in Fig. 5(c).

The 'M4' samples (four layers of skin) exhibit indentation type I failures for l values less than 80 mm, indentation type II failures for l between 80 mm and 140 mm, and tensile skin failures for l values greater than 140 mm. Behaviour patterns of peak load, P, are the same as for the 'M3' sandwiches for all three failure modes.

4.3. Failure Map

4.3.1. Experimental Failure Map

The experiments clearly show how the geometrical parameters l and t influence the failure mode of the sandwich structures studied in this work.

Downloaded by [Siauliu University Library] at 06:51 17 February 2013

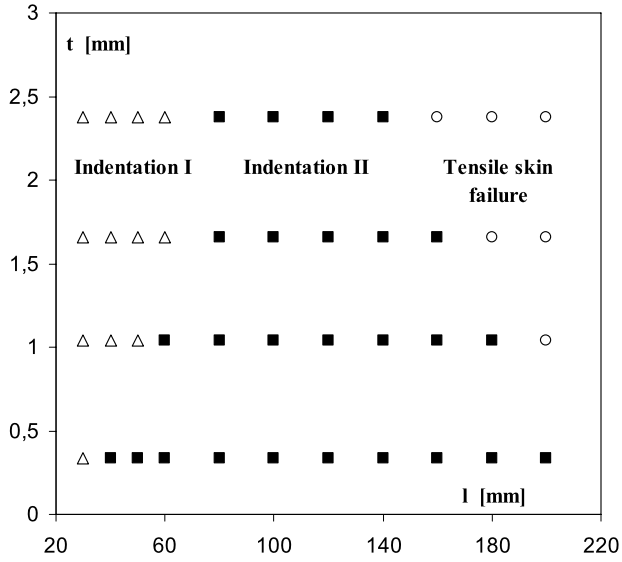

Figure 6. Experimental failure map of three point flexural test. (△) Indentation type I failure mechanism; (■) indentation type II failure mechanism; (○) tensile skin failure mechanism.

A failure map of l against t was created using the experimental results (Fig. 6). It shows the failure mode corresponding to each combination of l and t.

The map plainly shows the three regions in which each experimental failure mode is dominant.

For instance, for high values of l and t, only tensile skin failures occurred. Consequently, in this region of the map, tensile skin failure is the dominant mechanism.

With decreasing l or t, a transition between the tensile skin and indentation type II failures is observed.

For mid-values of l, indentation type II (for any value of t) becomes the dominant failure mechanism. This mid-value 'l' range widens as the corresponding value of t decreases. With decreasing l, a transition from indentation type II to indentation type I failure occurs. This point of transition happens at higher l values as the corresponding value of t increases.

At low values of l, indentation type I becomes the dominant failure mechanism.

4.3.2. Theoretical Model

From a theoretical point of view, a possible failure mechanism becomes the actual failure mechanism when its breaking load is lower than that of other competitive mechanisms.

Therefore, to determinate the theoretical curves that delimit the experimental regions of each failure mode, it is necessary to calculate when the fracture loads of the three mechanisms are equal. Using this approach, starting from their respective stress equations, the geometry governing the transition between failure modes can be ascertained.

For the tensile skin failure, it is possible to use equation (2).

Downloaded by [Siauliu University Library] at 06:51 17 February 2013

Downloaded by [Siauliu University Library] at 06:51 17 February 2013

Bearing in mind the two different types of indentation mechanism experimentally evidenced, we have taken two different theoretical equations for indentation in order to predict the experimental results. The first one is as proposed by Ashby *et al.* [13] and the second one by Fleck and Steeves [14].

The aim of using these equations is to create a theoretical model that can be used as a reliable tool to predict the failure mechanisms in sandwiches with defined geometry.

Ashby *et al.* [13] considered the indentation strength due to the combined plastic collapse of the skins and the core. They treat both the skins and the core as rigid, ideally plastic solids, with the core undergoing compressive yield and the skins forming plastic hinges.

By observing indentation type I as shown in Fig. 2, it can be noted that this particular experimental failure mode is very similar to that described by Ashby.

Therefore, the peak load for indentation type I failure is given in [13] by:

$$P_{\mathrm{I}} = 2 \cdot b \cdot t \cdot (\sigma_{\mathrm{C}} \cdot \sigma_{\mathrm{f}})^{1/2}. \tag{6}$$

In the work of Fleck and Steeves [14], it is shown experimentally and by finite element analysis that the indentation mode is due to the elastic deformation of the skin and the compressive yield of the core. Figure 3 shows that this description can be used to illustrate indentation type II as experimentally evidenced in this work.

Therefore, the value of indentation type II failure load is given in [14] by:

$$P_{\mathrm{II}} = b \cdot t \cdot \left(\frac{\pi^2 \cdot (t + c) \cdot E_{\mathrm{f}} \sigma_{\mathrm{C}}^2}{3 \cdot l} \right)^{1/3}. \tag{7}$$

By equating P_{I} to P_{II} we obtain the theoretical curve that delimits the experimental regions of the two types of indentation:

$$2 \cdot b \cdot t \cdot (\sigma_{\mathrm{C}} \cdot \sigma_{\mathrm{f}})^{1/2} = b \cdot t \cdot \left(\frac{\pi^2 \cdot (t + c) \cdot E_{\mathrm{f}} \sigma_{\mathrm{C}}^2}{3 \cdot l} \right)^{1/3}. \tag{8}$$

Rearranging gives the following equation:

$$t = A \cdot l - c, \tag{9}$$

with

$$A = \frac{24}{\pi^2} \cdot \frac{\sigma_{\mathrm{f}}^{3/2}}{\sigma_{\mathrm{C}}^{1/2}} \frac{1}{E_{\mathrm{f}}}. \tag{10}$$

In the same way, if we equate P_{II} to P_{ST} the indentation type II/tensile skin failure boundary is described:

$$b \cdot t \cdot \left(\frac{\pi^2 \cdot (t + c) \cdot E_{\mathrm{f}} \sigma_{\mathrm{C}}^2}{3 \cdot l} \right)^{1/3} = \frac{4 \cdot b \cdot t \cdot c \cdot \sigma_{\mathrm{f}}}{l}. \tag{11}$$

Rearranging gives the following equation:

$$t = \frac{B}{l^2} - c, \tag{12}$$

with

$$B = \frac{192 \cdot \sigma_f^3 \cdot c^3}{\pi^2 \cdot E_f \sigma_C^2}. \tag{13}$$

Consequently, the 'transition line' equations of the theoretical model are given by:

$$t = A \cdot l - c \quad \text{(transition from indentation type II — indentation type I)},$$
$$t = \frac{B}{l^2} - c \quad \text{(transition from indentation type II — tensile skin failure)},$$

with A and B as constants given by the following equations:

$$\begin{cases} A = \dfrac{24}{\pi^2} \cdot \dfrac{\sigma_f^{3/2}}{\sigma_C^{1/2}} \dfrac{1}{E_f} = 2.4317 \cdot \dfrac{\sigma_f^{3/2}}{\sigma_C^{1/2} \cdot E_f}, \\ B = \dfrac{192 \cdot \sigma_f^3 \cdot c^3}{\pi^2 \cdot E_f \cdot \sigma_C^2} = 2431.71 \cdot \dfrac{\sigma_f^3}{\sigma_C^2 \cdot E_f}. \end{cases} \tag{14}$$

In order to draw the theoretical transition curves it is necessary to know the values of following parameters: σ_f = tensile strength of skin, E_f = Young's modulus for skin, σ_C = core compressive strength. Core compressive strength, σ_C, as supplied by the producers, is equal to 0.85 MPa.

Five tensile tests (according to ASTM D3039 standard) were carried out to determinate the mechanical properties (E_f and σ_f) of the sandwich skins.

From these experimental tests the following values were obtained:

$$E_f = (26.72 \pm 0.11) \text{ GPa},$$
$$\sigma_f = (108.1 \pm 1.03) \text{ MPa}.$$

The theoretical model equations yield two transition lines when l is plotted against t. By mapping these theoretical results onto the failure map of experimental results as shown in Fig. 7, the results are unmistakably consistent.

From Fig. 7, it is evident that the two indentation mechanism types cover the majority of the map whereas tensile skin failure occurs in a limited area only.

This can be explained by the following theoretical point. The breaking loads of both indentation mechanisms are a function of core mechanical properties. Tensile skin failure breaking loads, however, are independent from these properties as seen in equation (2). Due to the poor mechanical performance of the PVC foam core used in this work (see Section 3.1), the breaking loads for indentation type fractures are lower than for tensile skin failures in a large number of the tested samples.

Tensile skin failure becomes dominant in the area of the map with high values of l and t. This result can be explained by considering that, for this geometrical configuration, the indentation resistance of the upper skin increases, preventing earlier indentation failure. Consequently, stress is transmitted to the inferior elements of the sandwich causing the axial stress to exceed the tensile strength of the lower skin.

Downloaded by [Siauliu University Library] at 06:51 17 February 2013

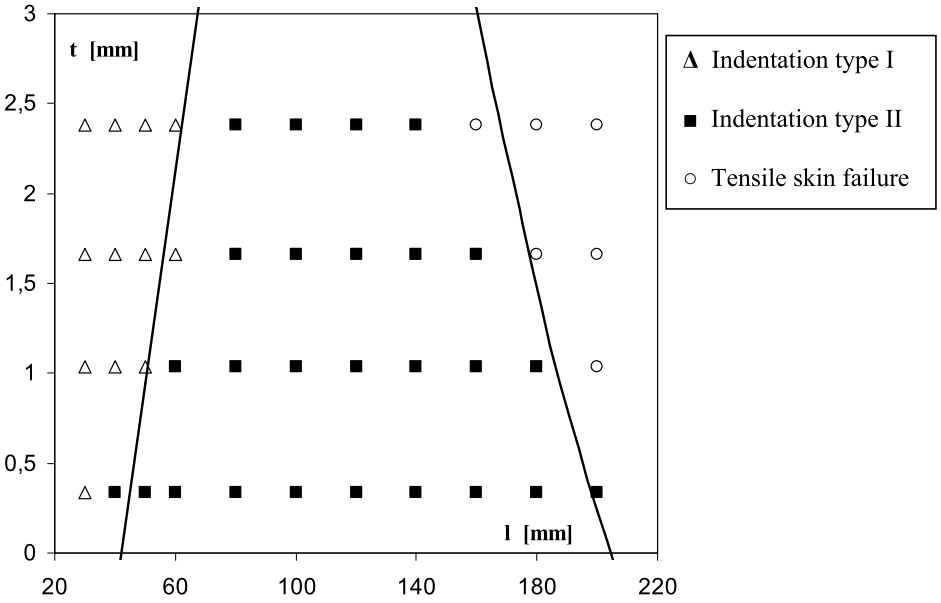

Figure 7. Failure map: comparison of theoretical curves and experimental data.

5. Conclusion

In this work, the failure mechanisms of E-glass mat/epoxy composite and closed-cell PVC foam cores sandwiches were investigated experimentally by three-point flexural tests. The study focused on the relationship between the failure modes and the geometrical parameters of skin thickness (t) and span length between supports (l) of the sandwich.

Four symmetrical sandwiches with a different number of layers (and consequently different thickness) were prepared and subject to three-point flexural tests. The span length between supports was varied from 30 mm to 200 mm.

The experimental tests show that, for the sandwich structures analysed in this work, only three failure mechanisms occur: two different types of indentation (called indentation type I and type II, respectively) and tensile skin failure.

In order to better evidence the experiments results, a failure map was created plotting failure mechanism on a graph of l against t.

A theoretical model was then created in order to optimize the use of these sandwich beams as structural elements. With this aim, two theoretical curves delimiting the regions of the experimental map were derived using fracture load equations for the three mechanisms as a starting point.

The theoretical model was consistent with the experimental results, and therefore represents a reliable tool to predict the failure mechanisms in sandwiches with defined geometry.

Downloaded by [Siauliu University Library] at 06:51 17 February 2013

References

1. R. Atkinson, Innovative uses for sandwich constructions, *Reinforced Plastics* **41**, 30–33 (1997).
2. G. Belingardi, M. P. Cavatorta and R. Duella, Material characterization of a composite–foam sandwich for the front structure of a high speed train, *Composite Structures* **61**, 13–25 (2003).
3. K. Branner, Capacity and lifetime of foam core sandwich structures, *PhD Thesis*, Department of Ocean Engineering, Technical University of Denmark, Lyngby, Denmark (1995).
4. C. A. Steeves and N. A. Fleck, Material Selection in sandwich beam construction, *Scripta Materialia* **50**, 1335–1339 (2004).
5. A. Petras and M. P. F. Sutcliffe, Failure mode maps for honeycomb sandwich panels, *Composite Structures* **44**, 237–252 (1999).
6. M. S. Konsta-Gdoutos and E. E. Gdoutos, The effect of load and geometry on the failure modes of sandwich beams, *Appl. Compos. Mater.* **12**, 165–176 (2005).
7. E. E. Gdoutos, I. M. Daniel and K. A. Wang, Compression facing wrinkling of composite sandwich structures, *Mech. Mater.* **35**, 511–522 (2003).
8. H. G. Allen, *Analysis and Design of Structural Sandwich Panels*. Pergamon Press, New York, USA (1969).
9. D. Zenkert, *An Introduction to Sandwich Construction*. Emas Publishing Ltd., London, UK (1995).
10. A. Petras and M. P. F. Sutcliffe, Indentation failure analysis of sandwich beams, *Composite Structures* **50**, 311–318 (2000).
11. V. Rizov, A. Shipsha and D. Zenkert, Indentation study of foam core sandwich composite panels, *Composite Structures* **69**, 95–102 (2005).
12. M. Styles, P. Compston and S. Kalyanasundaram, The effect of core thickness on the flexural behaviour of aluminium foam sandwich structures, *Composite Structures* **80**, 532–538 (2007).
13. M. F. Ashby, A. G. Evans, N. A. Fleck, L. J. Gibson, J. W. Hutchinson and H. N. G. Wadley, *Metal Foams: A Design Guide*. Butterworth Heinemann Publications, Oxford, UK (2000).
14. N. A. Fleck and C. A. Steeves, Collapse mechanisms of sandwich beams with composite faces and a foam core, loaded in three-point bending. Part I: Analytical models and minimum weight design, *Intl. J. Mech. Sci.* **46**, 561–583 (2004).

Downloaded by [Siauliu University Library] at 06:51 17 February 2013